Supporting Information

Reductive Transformation of 3-Nitro-1,2,4-triazol-5-one (NTO) by Leonardite Humic Acid and Anthraquinone-2,6-disulfonate (AQDS)

Jimmy Murillo-Gelvez[1], Dominic M. Di Toro[1], Herbert E. Allen[1], Richard F. Carbonaro[2,3], Pei C. Chiu[1]*

[1]Department of Civil and Environmental Engineering, University of Delaware, Newark, DE 19716

[2]Department of Chemical Engineering, Manhattan College, Riverdale, NY 10471

[3]Mutch Associates LLC, Ramsey, NJ 07446

[*]Corresponding Author Email: pei@udel.edu

Phone: +1 (302) 831-3104

Fax: +1 (302) 831-3640

Summary (17 Pages, 2 Tables, 11 Figures)

Section I. Materials and Methods.

Section II. Tables and Figures.

Section I. Materials and Methods.

Text S1. Chemicals.

NTO was obtained from ARDEC (Army Armament Research, Development and Engineering Center, Picatinny, NJ). NTO standards were acquired from AccuStandard (New Haven, CT). ATO (>99%) was purchased from Princeton BioMolecular Research (Princeton, NJ). AQDS (9,10-anthraquinone-2,6-disulfonic acid, disodium salt, 98%) was acquired from Combi Blocks (San Diego, CA) or TCI (Montgomeryville, PA). LHA (1S104H) was purchased from the International Humic Substances Society (IHSS, St. Paul, MN). Sodium dithionite ($Na_2S_2O_4$, >85%) and riboflavin 5'-monophosphate (sodium salt dihydrate, >75%) were acquired from Alfa Aesar (Haverhill, MA). 2-(4-Morpholino)ethane sulfonic acid (MES, >98%), sodium hydroxide (1 N solution), sodium sulfite (Na_2SO_3, anhydrous, ≥98%), sodium sulfate (Na_2SO_4, anhydrous, ≥99%), potassium hydroxide (≥85%), and hydrochloric acid (38%) were obtained from Fisher Scientific (Pittsburgh, PA). 2-Amino-2-(hydroxymethyl)-1,3-propanediol (Tris, 99.8%), 1,1′-ethylene-2,2′-bipyridyldiylium dibromide (diquat, monohydrate, >99%), and 7-hydroxy-3H-phenoxazin-3-one (resorufin, sodium salt, >99%) were purchased from Sigma-Aldrich (St. Louis, MO). 3-Cyclohexylamino-2-hydroxy-1-propanesulfonic acid (CAPSO, >99%) was obtained from Bio-Rad Laboratories (Hercules, CA). Potassium ferricyanide ($K_3Fe(CN)_6$, >99%) and hexaammineruthenium(III) chloride ($Ru(NH_3)_6Cl_3$, 98%) were purchased from ACROS Organics (Morris Plains, NJ). Zobell's solution was obtained from LabChem (Zelienople, PA). All chemicals were used as received.

Text S2. Analytical Methods

NTO and ATO were analyzed using an Agilent 1200 Series high performance liquid chromatograph (HPLC, Agilent, Santa Clara, CA) with an Agilent 1260 diode array detector (DAD). The HPLC was equipped with a Thermo Scientific (Waltham, MA) Hypercarb™ Porous Graphitic Carbon column (100 × 4.6 mm, 5 μm particle size). The injection volume was 100 μL. The eluents were 0.1% trifluoroacetic acid (TFA) and acetonitrile in the following gradient: 100% TFA (0–1.5 min), 85% TFA (1.5–6.5 min), 50% TFA (6.5–8.5 min), and 100% TFA (8.5–10.0 min). The flow rate was 2.0 mL/min, the run time was 10 min, and the temperature was constant at 34.0 °C. NTO and ATO were detected at 7.9 min (318 nm) and 4.3 min (210 nm). The response factor for ATO at pH 10 was lower than that at pH 8.0 and 6.5 (Figure S1), presumably due to deprotonation (pK_a = 8.789 ± 0.022, determined following previously published methods[1]), and thus a separate calibration curve was prepared for pH 10.

pH was measured using an Oakton pH electrode (Oakton Instruments, Vernon Hills, IL) calibrated with pH 4, 7, and 10 standards. Reduction potential was measured using an ORP electrode InLab Redox Micro with platinum ring (Part #51343203, Mettler Toledo, Columbus, OH) and an Orion Dual Star meter (Thermo Scientific). The ORP electrode was calibrated periodically against the Zobell's solution.

Sulfite and sulfate were quantified using a Metrohm 940 Professional IC Vario System. The eluent was a mixture of 3.2 mM sodium carbonate, 1 mM sodium bicarbonate, and 6.5% (v/v) acetone. The flow rate was 1.5 mL/min, the run time 12 min, and the temperature 28 °C. A mixture of sulfuric acid and methanol was used to rinse and regenerate the suppressor.

Section II. Tables and Figures.

Table S1. Names, structures, numbers of electrons and protons transferred, reduction potentials, and covered reduction potential ranges of the mediators used for measuring LHA redox potential profile via mediated potentiometry.

Mediator Name	Oxidized Species	ne^- / nH^+	Reduced Species	$E_H^{0'}$ $(mV)^a$	E_H Range (mV)^b
Hexaammineruthenium	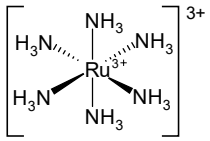	$\overset{+e^-}{\underset{-e^-}{\longleftrightarrow}}$	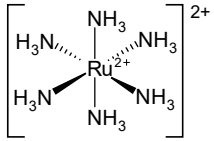	+90	+210 to -30
Resorufin (7-Hydroxy-3*H*-phenoxazin-3-one)	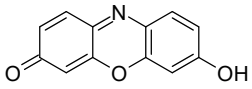	$\overset{+2e^-+2H^+}{\underset{-2e^--2H^+}{\longleftrightarrow}}$	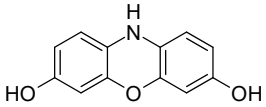	-30	+30 to -90
Riboflavin 5'-monophosphate	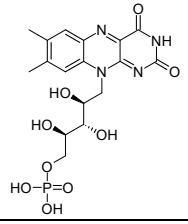	$\overset{+2e^-+2H^+}{\underset{-2e^--2H^+}{\longleftrightarrow}}$	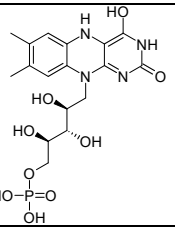	-180	-120 to -240
Diquat	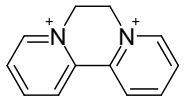	$\overset{+e^-}{\underset{-e^-}{\longleftrightarrow}}$	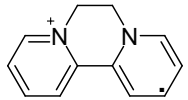	-350	-230 to -470

[a] Reduction potentials at pH 7.0.[2] [b] Range of useful reduction potentials: ±60 mV for 2 e^- and ±120 mV for 1 e^- transfer mediators.[2]

Table S2. Observed pseudo-first-order rate constants (k_{Obs}) for NTO reduction by $AQDS_{Red}$ at different pH. k_{Obs} values are the mean of replicate reactors ± one standard deviation.

pH	k_{Obs} (s^{-1})	$\log k_{Obs}$ (s^{-1})	Number of Replicates
1.486	$(2.62 \pm 0.02) \times 10^{-3}$	-2.581	2
1.994 ± 0.051	$(4.16 \pm 0.46) \times 10^{-3}$	-2.381	4
2.438	$(8.85 \pm 0.50) \times 10^{-3}$	-2.053	2
3.008 ± 0.004	$(1.95 \pm 0.29) \times 10^{-2}$	-1.710	4
3.500	$(4.30 \pm 0.21) \times 10^{-2}$	-1.367	2
4.011 ± 0.035	$(4.76 \pm 0.83) \times 10^{-2}$	-1.322	4
4.487	$(5.78 \pm 0.37) \times 10^{-2}$	-1.238	2
5.038 ± 0.053	$(5.28 \pm 0.53) \times 10^{-2}$	-1.277	4
5.997	$(5.80 \pm 0.37) \times 10^{-2}$	-1.237	2
6.491 ± 0.060	$(5.26 \pm 0.15) \times 10^{-2}$	-1.279	4
7.015 ± 0.022	$(5.92 \pm 0.78) \times 10^{-2}$	-1.227	6
8.020 ± 0.029	$(5.02 \pm 0.50) \times 10^{-2}$	-1.299	6
8.987 ± 0.073	$(4.67 \pm 0.34) \times 10^{-2}$	-1.331	6
9.529 ± 0.063	$(4.59 \pm 0.42) \times 10^{-2}$	-1.338	6
10.052 ± 0.063	$(4.27 \pm 0.71) \times 10^{-2}$	-1.369	4
10.506 ± 0.008	$(3.81 \pm 0.31) \times 10^{-2}$	-1.419	4
10.998 ± 0.082	$(1.71 \pm 0.16) \times 10^{-2}$	-1.766	6
11.552 ± 0.042	$(4.18 \pm 0.52) \times 10^{-3}$	-2.378	4
12.050 ± 0.046	$(4.49 \pm 1.61) \times 10^{-4}$	-3.348	6
12.535	$(3.16 \pm 0.01) \times 10^{-5}$	-4.501	2

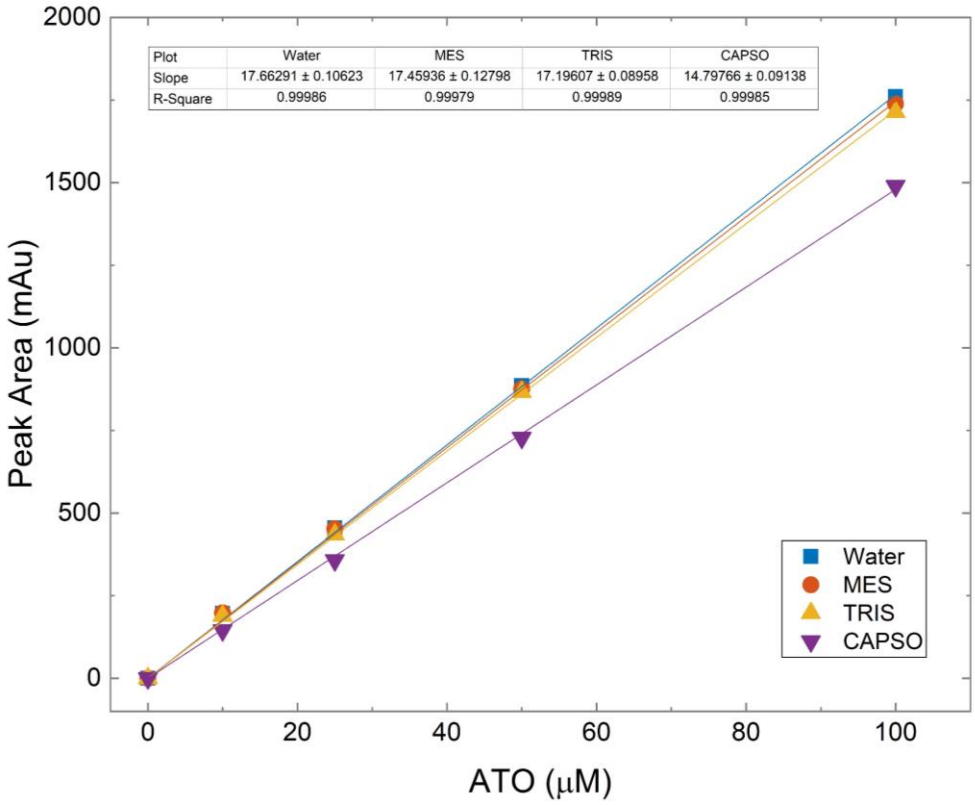

Figure S1. Calibration curves of ATO in water and 50 mM MES, Tris, or CAPSO buffer. The pH in MES, Tris, and CAPSO solutions was 6.5, 8.0, and 10.0, respectively. The inset gives the slopes and R^2 values of the calibration curves. Note the slope (response factor) changes most noticeably between pH 8 and 10.

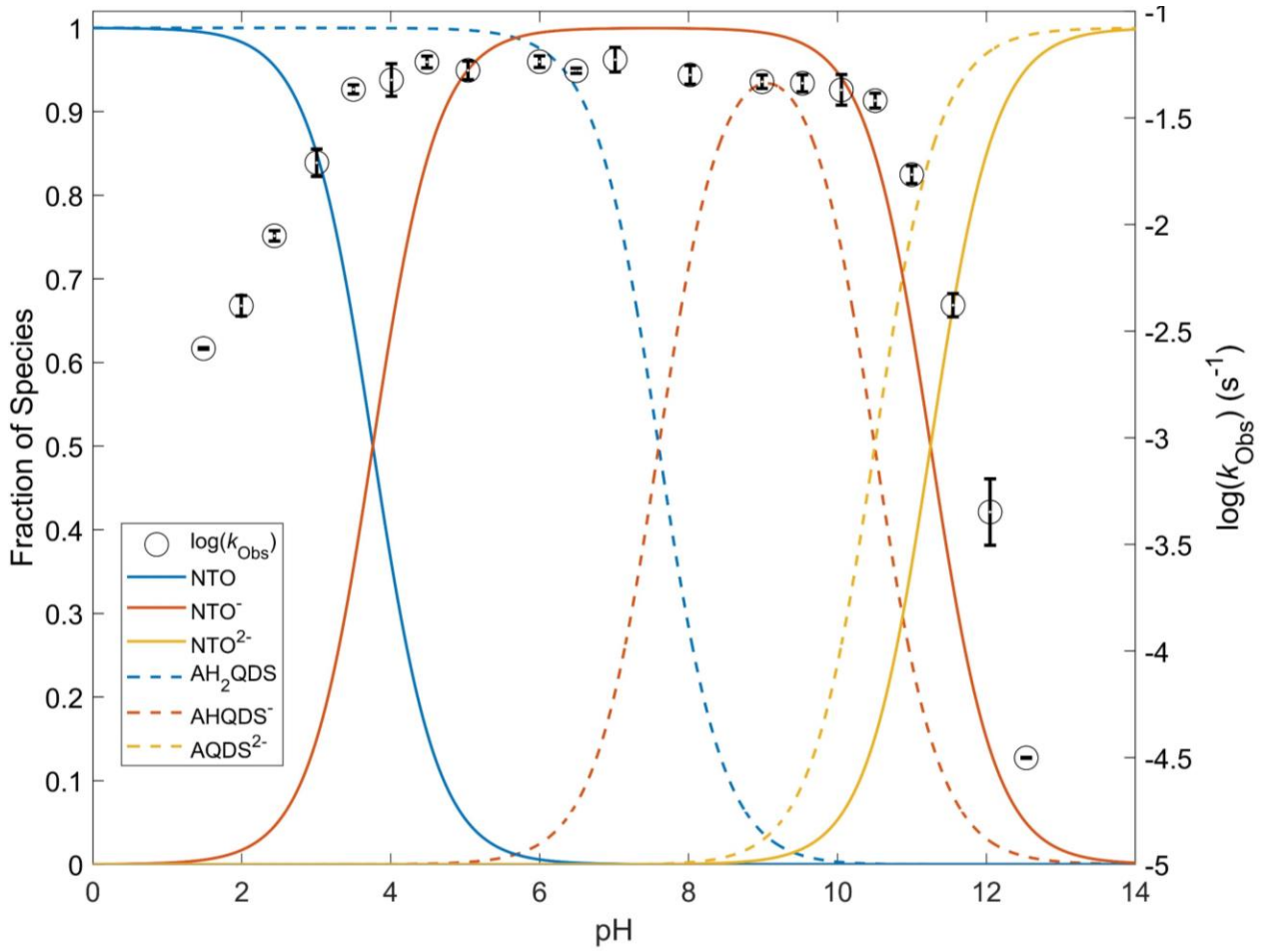

Figure S2. Speciation of NTO and AH_2QDS as a function of pH and its relation to the observed pseudo-first order reaction rate constants (k_{Obs}). The fractions (α values) were computed using the reported $pK_{a,1}$ and $pK_{a,2}$.[3,4] Solid and dashed lines correspond to NTO and AH_2QDS species, respectively. Error bars represent ± 1 standard deviation based on replicate reactors.

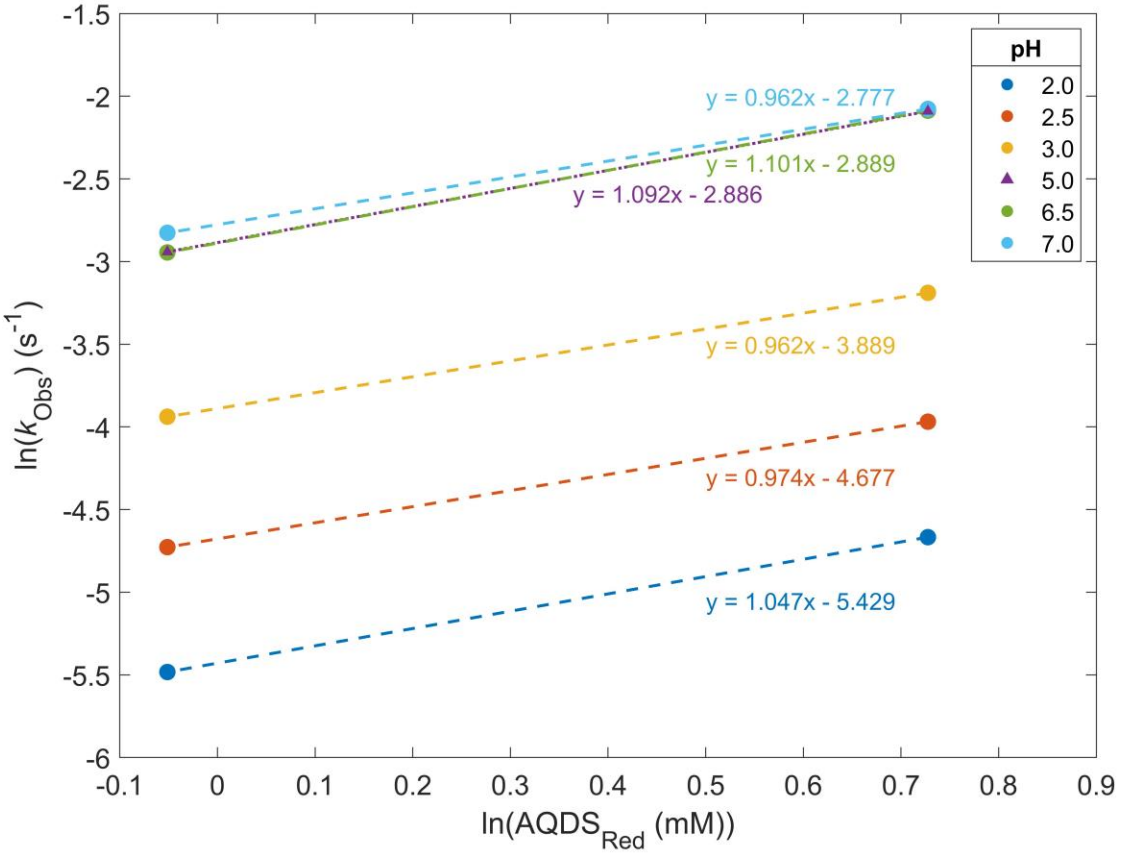

Figure S3. Dependency of k_{Obs} on the concentration of $AQDS_{Red}$. The data points represent rate constants measured at different pH having a total $AQDS_{Red}$ concentrations of 0.95 or 2.07 mM. The fitted reaction order with respect to [$AQDS_{Red}$] using all the data points was 1.023 ± 0.065.

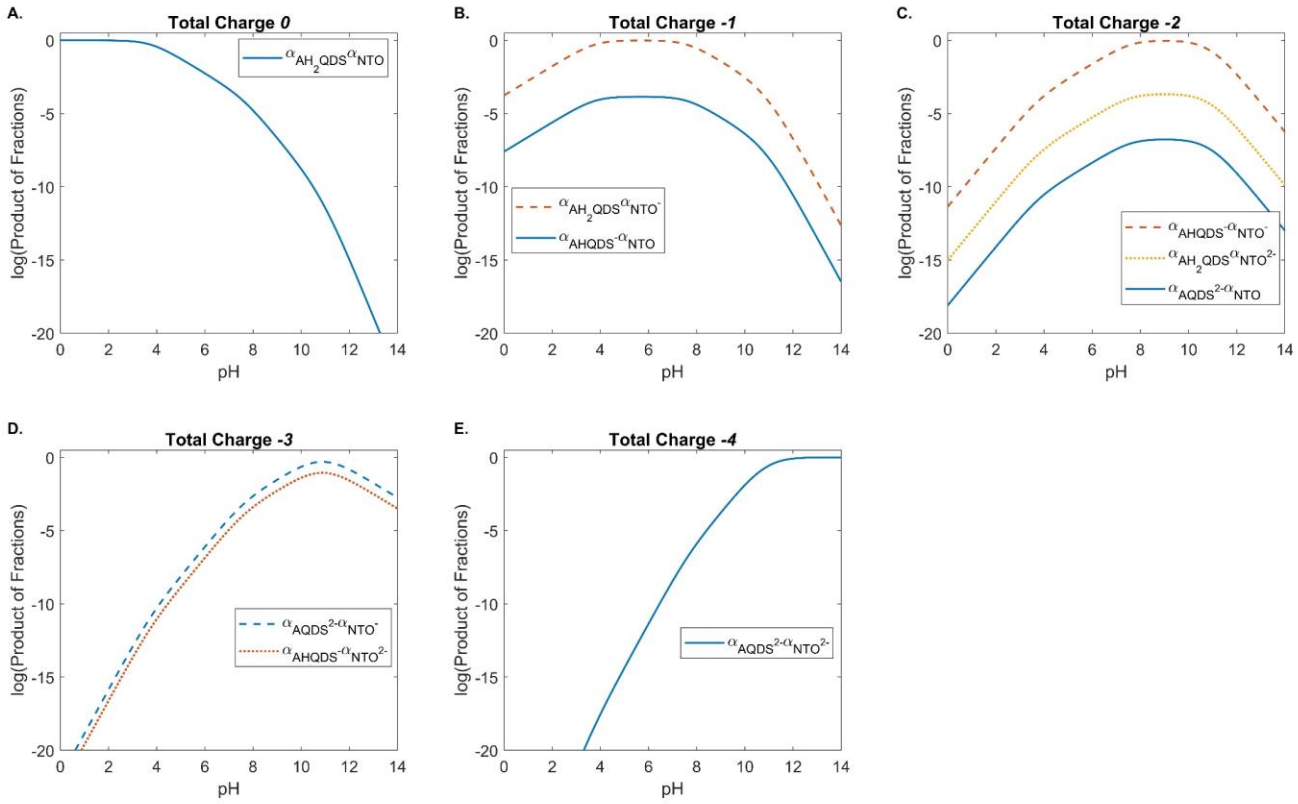

Figure S4. Product of fractions as a function of pH for the five total charge groups of different pairs of reactant species. Product of fractions (α values) for **A.** AH_2QDS and NTO. Total charge of 0. **B.** AH_2QDS and NTO^-, and $AHQDS^-$and NTO. Total charge of -1. **C.** $AHQDS^-$ and NTO^-, AH_2QDS and NTO^{2-}, and $AQDS^{2-}$ and NTO. Total charge of -2. **D.** $AQDS^{2-}$ and NTO^-, and $AHQDS^-$ and NTO^{2-}. Total charge of -3. **E.** $AQDS^{2-}$ and NTO^{2-}. Total charge of -4. The fractions were computed using the reported $pK_{a,1}$ and $pK_{a,2}$ of both reactants.[3,4] Note that the charges of the two sulfonate groups of AH_2QDS are not included.

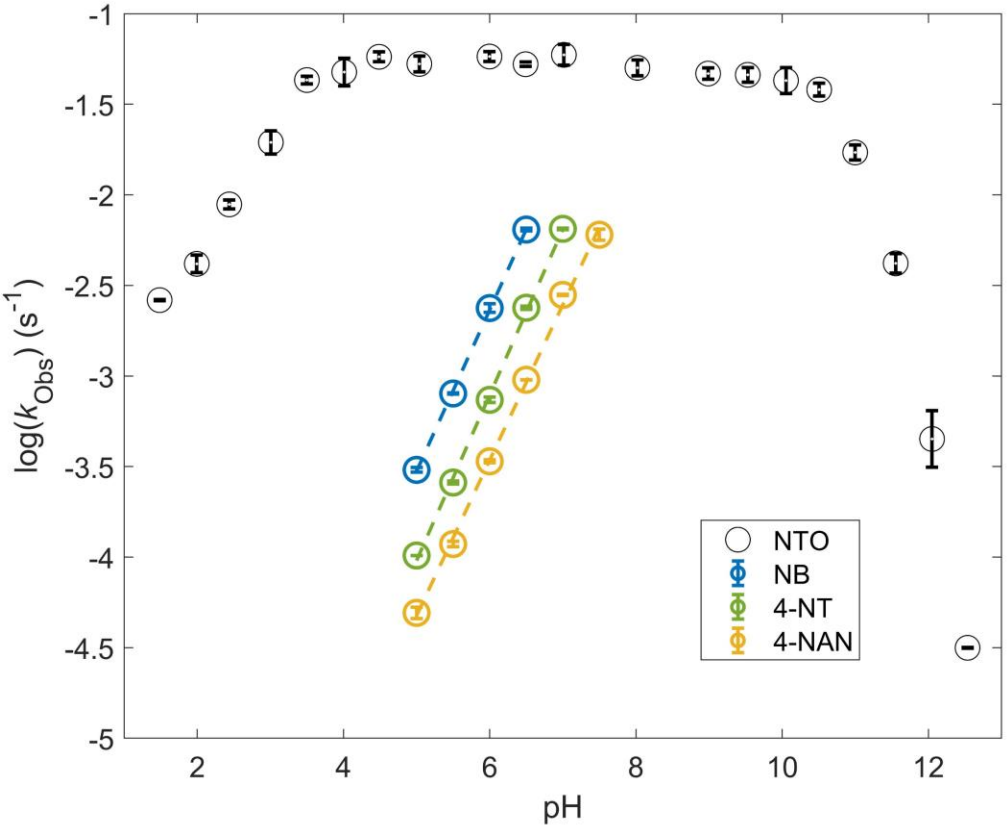

Figure S5. Observed reduction rate constants for NTO and neutral NACs with ~1 mM $AQDS_{Red}$ as a function of pH. The data for nitrobenzene (NB), 4-nitrotoluene (4-NT), and 4-nitroanisole (4-NAN) was taken from a previous study.[5] The dashed lines are the least squares fits of the (substituted) nitrobenzene data. The obtained slopes were 0.86 – 0.92 for all three NBs, suggesting that the increasing concentration of $[AHQDS^-]$ caused the rise in k_{Obs}.

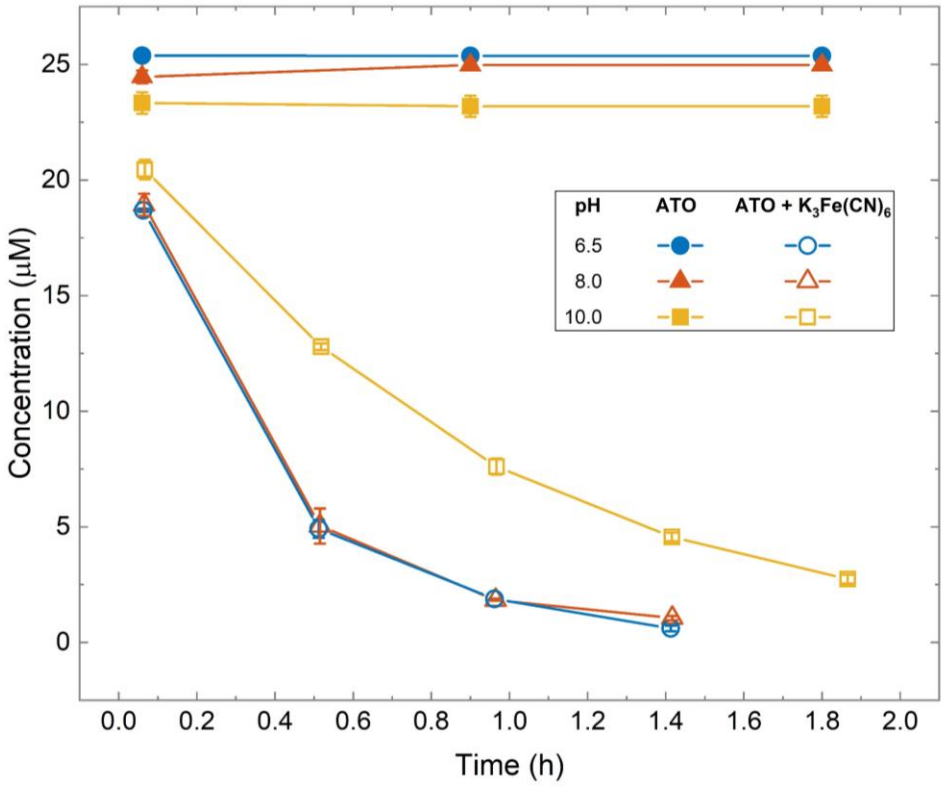

Figure S6. Decrease of ATO concentration as a function of time in the presence of potassium ferricyanide at three different pH conditions. The buffers used were MES (pH 6.5), TRIS (pH 8.0), and CAPSO (pH 10.0) at a total concentration of 50 mM. ATO was stable in buffer solutions without ferricyanide (filled markers). Data represent means of duplicate reactors and error bars ± one standard deviation.

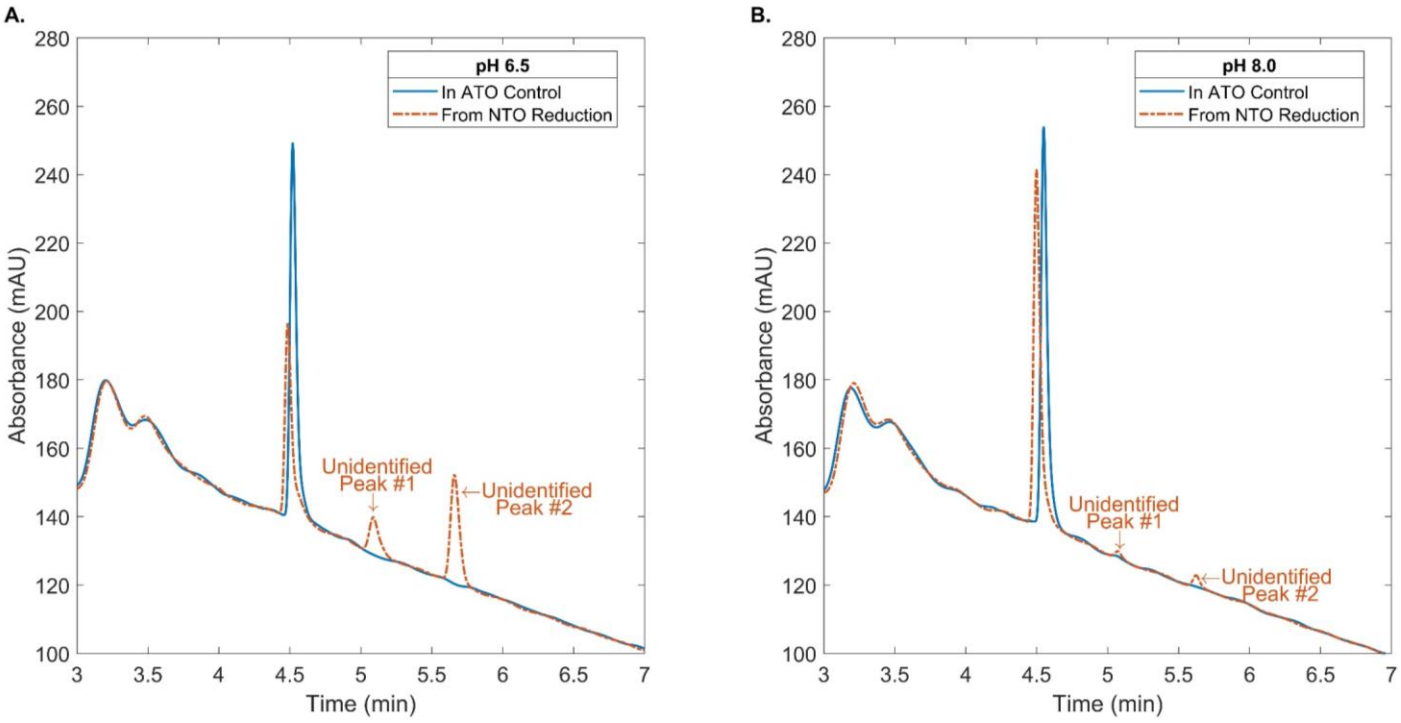

Figure S7. Chromatograms of samples from reactors at **A.** pH 6.5 (50 mM MES buffer) and **B.** pH 8.0 (50 mM TRIS buffer) initially containing 0.9 mM $AQDS_{Red}$, and either 20 µM ATO (solid blue line) or 20 µM NTO (orange dotted line). Note that the peaks from NTO reactors correspond to NTO reduction products, which include ATO (at ~4.5 min) and two unidentified products.

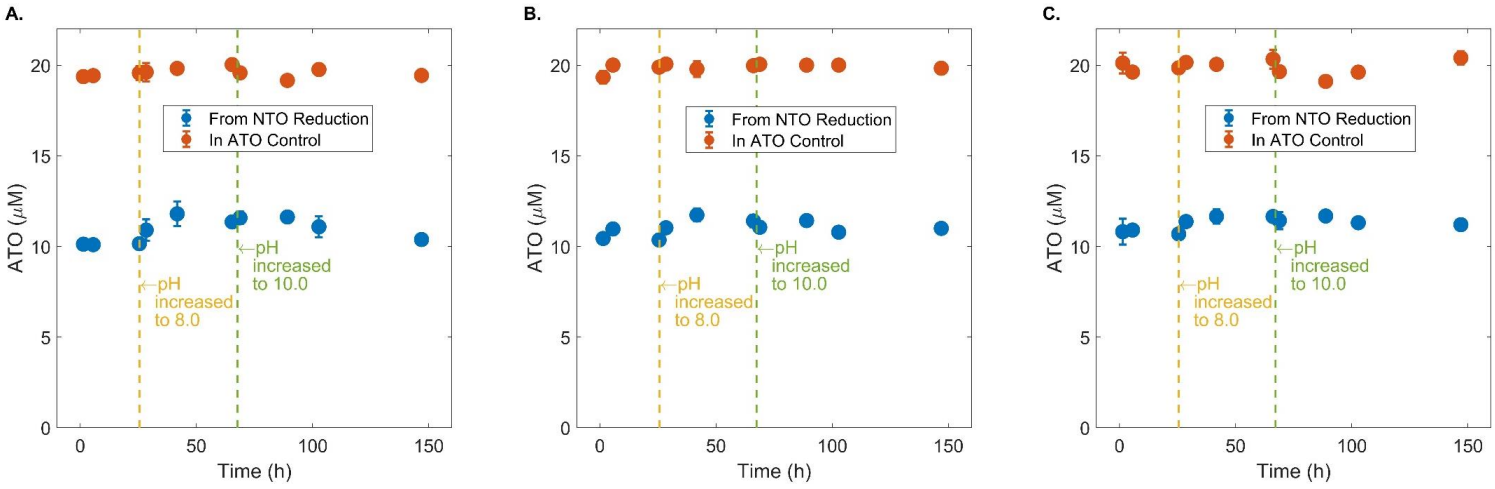

Figure S8. ATO produced from NTO (blue circles) and present in controls (red circles) in reactors containing 0.9 mM $AQDS_{Red}$ at pH **A.** 2.0, **B.** 4.0, and **C.** 6.5. The vertical dashed lines represent the times when the pH of the reactors was increased to the indicated values. Concentrations are the mean of duplicate reactors; error bars represent ± one standard deviation.

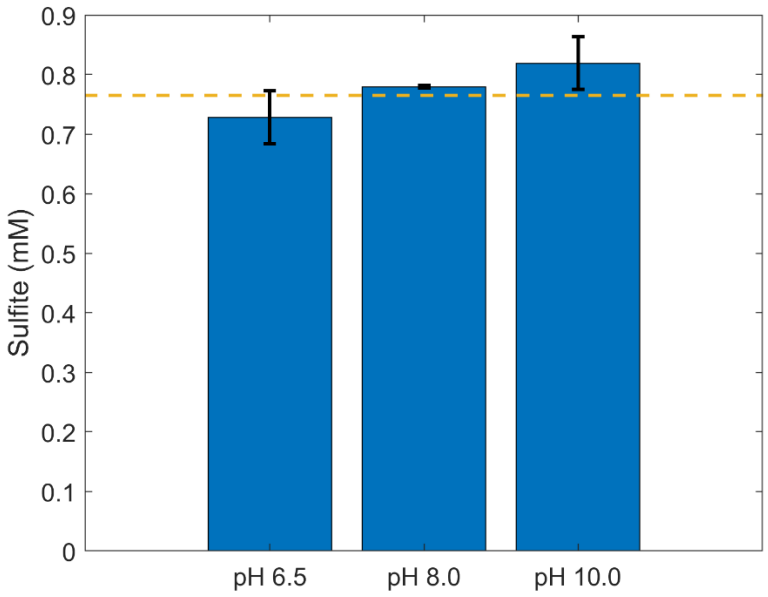

Figure S9. Sulfite concentrations in LHA_{Red} reactors (0.5 g/L) 30 days after dithionite addition. The yellow dashed line indicates the expected sulfite concentration based on the amount of dithionite added and Eq. 4. Error bars represent ± one standard deviation from triplicate measurements.

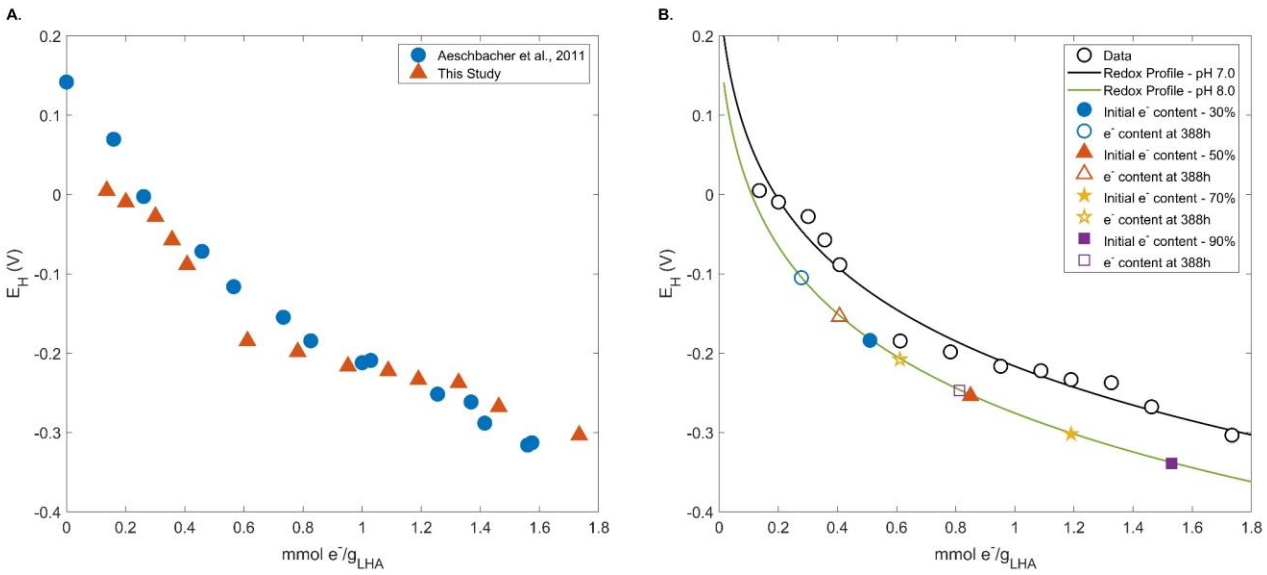

Figure S10. A. Redox potential profile of Leonardite humic acid measured at pH 7.0 in 0.1 M phosphate buffer. Reactors were incubated for at least 24 h after dithionite addition before a redox mediator was spiked and E_H measured. E_H values are relative to SHE. The redox mediators used and the redox potential ranges covered are detailed in Materials and Methods and Table S1. For comparison, the blue circles are data taken from Aeschbacher et al. where LHA was reduced electrochemically at pH 7.0 in 0.1 M phosphate buffer and E_H measured via mediated potentiometry.[6] **B.** Fitted redox potential profile of LHA (solid black line) using the titration data (black circles) and Eq. S1 below. The redox potential profile at pH 8.0 (solid green line) was obtained by subtracting 60 mV from the pH 7.0 profile.[6] Colored markers on the pH 8.0 curve indicate the redox states of the initial (filled markers, before NTO addition) and remaining (hollow markers, after 388 h of reaction) electron contents of the reactors shown in Figure 5.

Equation S1 is the exponential function used to fit the titration data, which has been used previously for the same purpose.[6]

$$n_{e^-} = a + b\ exp^{-c(E_H)} + j\ exp^{-k(E_H)} + p\ exp^{-q(E_H)} \quad \text{(S1)}$$

where a, b, c, j, k, p, and q are the fitting parameters, E_H (y axis) is the measured reduction potential at a given pH and extent of reduction, and n_{e^-} is the amount of electrons added to LHA in $\frac{mmol\ e^-}{g_{LHA}}$ (x axis).

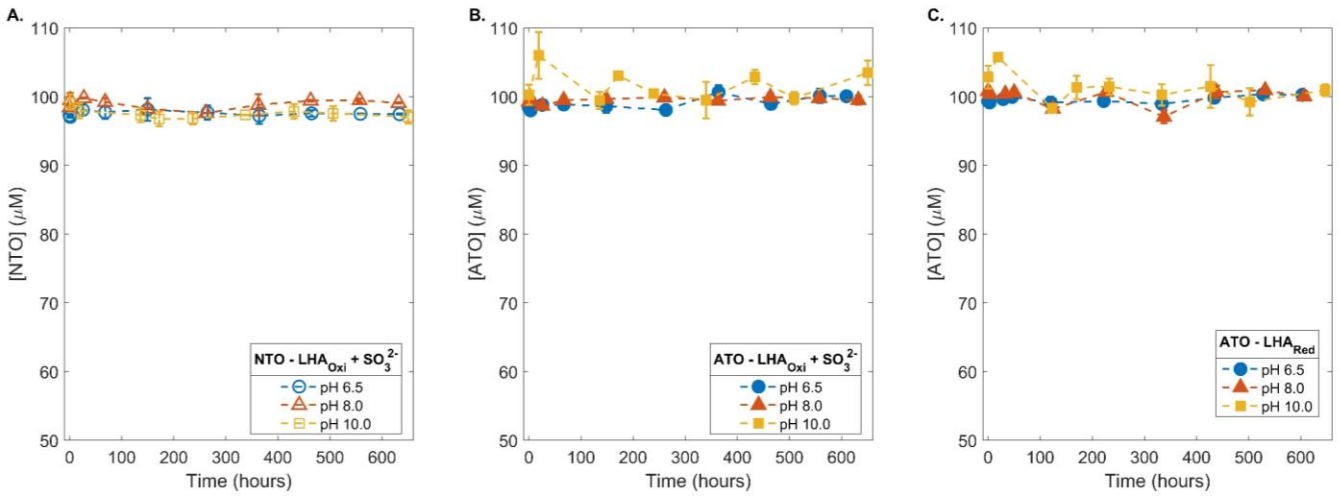

Figure S11. A. Stability of NTO in the presence of air-oxidized LHA (LHA_{Oxi}) and 0.765 mM sulfite (SO_3^{2-}) over 650 h. **B.** Stability of ATO in the presence of LHA_{Oxi} and 0.765 mM SO_3^{2-} over 650 h. **C.** Stability of ATO in the presence of reduced LHA (LHA_{Red}) and 0.765 mM sulfite (produced from dithionite oxidation). Each data point represents the mean from duplicate reactors. Error bars show ± one standard deviation.

References

(1) Albert, A.; Serjeant, E. P. *The Determination of Ionization Constants: A Laboratory Manual*; Springer Netherlands, 2012.

(2) Sander, M.; Hofstetter, T. B.; Gorski, C. A. Electrochemical Analyses of Redox-Active Iron Minerals: A Review of Nonmediated and Mediated Approaches. *Environ. Sci. Technol.* **2015**, *49* (10), 5862–5878. https://doi.org/10.1021/acs.est.5b00006.

(3) Kofman, T. P.; Pevzner, M. S.; Zhukova, L. N.; Kravchenko, T. A.; Frolova, G. M. Methylation of 3-Nitro-1,2,4-Triazol-5-One. *Zhurnal Org. khimii* **1980**, *16* (2), 420–425.

(4) Gamage, R. S. K. A.; McQuillan, A. J.; Peake, B. M. Ultraviolet–Visible and Electron Paramagnetic Resonance Spectroelectrochemical Studies of the Reduction Products of Some Anthraquinone Sulphonates in Aqueous Solutions. *J. Chem. Soc. Faraday Trans.* **1991**, *87* (22), 3653–3660. https://doi.org/10.1039/FT9918703653.

(5) Murillo-Gelvez, J.; Hickey, K. P.; Di Toro, D. M.; Allen, H. E.; Carbonaro, R. F.; Chiu, P. C. Experimental Validation of Hydrogen Atom Transfer Gibbs Free Energy as a Predictor of Nitroaromatic Reduction Rate Constants. *Environ. Sci. Technol.* **2019**, *53* (10), 5816–5827. https://doi.org/10.1021/acs.est.9b00910.

(6) Aeschbacher, M.; Vergari, D.; Schwarzenbach, R. P.; Sander, M. Electrochemical Analysis of Proton and Electron Transfer Equilibria of the Reducible Moieties in Humic Acids. *Environ. Sci. Technol.* **2011**, *45* (19), 8385–8394. https://doi.org/10.1021/es201981g.